Measuring the thermal resistance of double and triple layer pneumatic cushions for textile architectures

Andrea Alongi[ad], Adriana Angelotti[ad]*, Alessandro Rizzo[b], Alessandra Zanelli[cd]

[a]*Energy Department, Politecnico di Milano, v. Lambruschini 4A, Milano 20156, Italy;* [b]*canobbio textile engineering srl, Strada Sgarbazzolo, Castelnuovo Scrivia (AL) 15053, Italy;* [c]*ABC Department, Politecnico di Milano, v. Bonardi 3, Milano 21033, Italy;* [d] *Textiles Hub, Politecnico di Milano, v. Ponzio 33, Milano 20133, Italy*

*corresponding author: adriana.angelotti@polimi.it

Abstract

Lightweight architecture, implementing coated fabric and membrane materials, increasingly adopts double or multiple layer pneumatic cushions. The reason lies in the possibility to guarantee adequate thermal insulation and better indoor comfort, especially in permanent buildings. The cushion thermal transmittance decreases as the number of layers increases. However, the U-value is generally assessed by simple calculations assuming the cushion layers are parallel planes. This way, the center-of-the cushion U-value is taken as the overall U-value, disregarding any effect of the curved geometry of the cushion on the heat transfer across it.

In this paper an experimental approach to the evaluation of the overall U-value of multiple layer cushions is proposed. Two sample cushions made up of PVC coated polyester with a surface of about 1 m^2 are built, one double layer and one triple layer. They are tested in vertical position in a double thermal chamber laboratory apparatus, establishing a constant temperature difference equal to 25°C across them. The cushion surfaces exposed to the chambers are divided into thermally homogeneous portions where temperature and heat flow density probes are centrally placed. This way the overall thermal resistance and thermal transmittance of the cushions are measured. In parallel, the U-value for the two samples are calculated using literature correlations for free convection in rectangular cavities and assuming radiative heat transfer between parallel grey surfaces. The experimental results show that, passing from two to three layers, the overall thermal resistance of the cushion almost doubles (+ 91%) and the thermal transmittance reduces by about 30%. At the same time, simple calculations of the U-value are found to underestimate the insulation capacity of the cushions, especially for the double layer one. These outcomes point out the necessity of further investigations to understand the impact of the cushion shape on free convection in the air cavity.

Keywords: pneumatic cushion, thermal resistance, thermal transmittance, energy performance, measurement, heat flow, free convection, multi-layered membrane skin.

1. Introduction

Pneumatic cushions are widely adopted in the so-called textile architecture with a variety of multilayered solutions, composed of 2 up to 5 layers to increase the thermal insulation: the resulting air gaps are inflated to an extra-pressure of 200-300 Pa up to 600-900 Pa. As far as materials are concerned, coated textiles, like PVC coated polyester, or Fluor polymeric foils, like ETFE, can be used. The first is generally preferred when disassembly and reassembly are foreseen, since the material can be folded many times without damaging. Therefore PES/PVC cushions are mainly found in temporary use installations, such as seasonal covers for sports halls (Suo et al. 2015), or in adaptable textile envelopes, such as the Chianciano Terme Pavillion by P. Bodega. Conversely ETFE is preferred when a highly transparent solution is required, so that ETFE is often considered a lightweight alternative to glass for roofs and atria (Robinson-Gayle et al. 2001). However, the very high solar transmission (Liu et al., 2016) can cause overheating in summer, so that ink printing and more recently so-called 3D printing (Cremers and Marx, 2017), are proposed to better control solar gains. Photovoltaics can also be integrated into transparent ETFE cushions (Hu et al. 2015; Hu et al., 2016). In this regard, the testing carried out on a triple layer ETFE cushion in summer conditions performed by (Hu et al. 2014) shows that integrating Amorphous Silicon PV cells in the middle layer does not compromise the structural behavior of the bottom and top ETFE layers and allows to effectively produce electricity and collect thermal energy.

Cushions can be shaped with a quite high freedom by architects, while the manufacture optimization suggests adopting rectangular shapes, with a span of 3 meters and an almost infinite development in the other direction (Gomez-Gonzalez et al., 2011; Le Cuyer, 2008). The fundamental thermal-physical properties of the cushion for evaluating the energy behavior of the textile envelope (Afrin et al. 2015) are the thermal transmittance (i.e. the *U*-

value) and the solar gain factor (i.e. *g*-value). The cushion thermal transmittance depends, besides on the number of layers, also on the heat flow direction (horizontal, upwards or downwards) that influences the natural convection in the air gaps. According to (Knippers et al., 2010), the center-of-the cushion thermal transmittance can be estimated in a roughly similar way both with CEN EN ISO 6946 and CEN EN 673, although none of the two is able to catch the non-steady state heat transfer mechanism connected to free convection inside the air cavities. Following the standards calculations, for the horizontal heat flow direction, passing from a double layer cushion to a triple layer allows to reduce the wintertime *U*-value from about 3 W/(m^{2}K) to about 2 W/(m^{2}K).

Actually, the center-of-the cushion *U*-value, representing the portion where the layers are almost planar and parallel, does not take into account the impact of the curved shape of the cushion. According to Flor et al. (2019), the experimental determination of the thermal performance appears to deliver a more realistic approach to provide data for a comprehensive energy simulation. Mainini et al. (Mainini et al., 2011) measure the thermal conductance of a double layer panel (dimensions: 1050 x 1140 mm) realized with two ETFE membranes, finding a conductance equal to $C = 5.158$ W/(m^{2}K) and a transmittance equal to $U = 2.748$ W/(m^{2}K). However, the two layers are parallel to each other and tensioned on an aluminum frame with no thermal break, therefore the effects of the typical curvature of the cushion are not considered. Flor et al. (Flor et al. 2019) evaluate in a climatic chamber the thermal performance of different ETFE cushions, where design variations include the number of layers, the presence of silver ink frits and the possibility to change the position of the central layer. They find a better performance for the triple layer cushion with frits/open configuration, followed by the double layer with frits, by the triple layer with frits/closed configuration and then by the double layer clear. However, since the heat flux across the cushion is measured only in three positions along the vertical axis in the center of the surfaces, it may be argued

that the effects of the cushion curvature on the thermal performance are only partially detected and coherently the U-value is not given.

Suo et al. (Suo et al. 2015) simulate the energy performance of different air-supported membranes for sports halls, namely single layer, double layer based on cushions and double layer with a slightly ventilated air cavity. As far as the double layer cushions simulation is concerned, the impact of thermal bridges on the center-of-the cushion thermal transmittance is firstly estimated by simplified 2D heat transfer simulations in THERM, resulting in an average extra heat flux equal to 9% on the hall envelope surface. Then the double cushions are modelled by means of an equivalent stratigraphy made up of an external fabric layer, an air gap layer and an internal fabric layer. The air gap thermal resistance is thus adjusted in order to achieve the overall U-value, including the increase due to thermal bridges.

In turn in (Antretter et al., 2008) 2D CFD simulations on a large size double layer ETFE cushion with realistic curvature are performed, with the aim to study the flow patterns inside the cavity. For inclined cushions, one big vortex is found with secondary flows in the upper and lower edges. For the horizontal cushion with heat flow upwards, several eddies are found, determining a good mixing in the cavity, apart from the edges.
As far as literature correlations for calculating the free convection heat coefficient in an enclosure are concerned (Ostrach, 1972; Incropera et al., 2007), they are only partially applicable to the cushion case, since: 1) they assume the rectangular cavity geometry, either vertical, horizontal or inclined at a given angle, 2) boundary conditions on two opposite sides of the cavity are expressed by uniform surface temperatures and 3) the cavity width is generally assumed to be very large compared to height and thickness, namely the geometry is bi-dimensional.

Therefore, further efforts are necessary to understand the heat transfer across cushions,

including natural convection in the curved cavities, and then evaluate U-values more accurately than with present parallel planes assumptions.

In this paper an experimental approach to the evaluation of the thermal resistance of different pneumatic cushions is adopted. A series of experimental tests are performed in a laboratory apparatus on two pneumatic cushion samples of small size, namely a double layer and a triple layer with vertical orientation. Collected data are processed to derive the thermal resistance and the thermal transmittance of each sample. The measured energy performances of the two cushions are then compared with each other. In the end, experimental outcomes are compared to values obtained using literature correlations for free convection in vertical cavities and radiative heat transfer between parallel grey planes.

2. The experimental setup

The tests are carried out in the laboratory rig called Dual Air Vented Thermal Box (DAVTB), developed at the Building Physics Laboratory of the Energy Department of Politecnico di Milano. This setup is designed to test building envelope technologies under user-defined thermal boundary conditions (both in steady and unsteady state) and, if needed, to force an airflow through permeable components such as Breathing Walls. For the purpose of this study, the air flow loop is not used. A detailed description of the apparatus and its features can be found in (Alongi et al. 2017, Alongi et al. 2020).

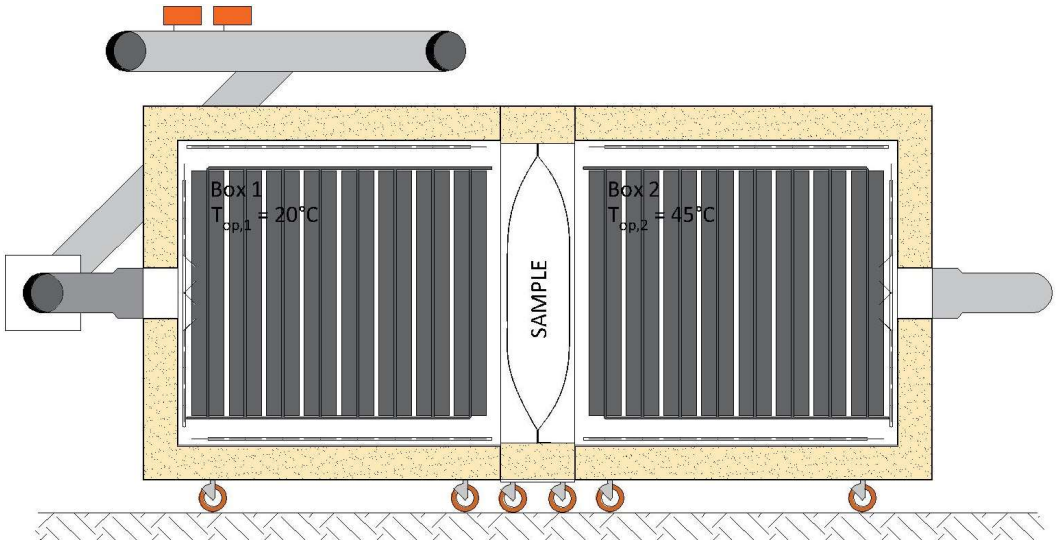

Figure 1: vertical section of the DAVTB apparatus. The radiant panels are visible both in Box 1 (left) and in Box 2 (right). The operative conditions adopted in this work are also reported, along with the cross section of one of the two samples experimentally investigated.

The DAVTB facility (Figure 1) consists of two insulated chambers (1.5 m x 1.5 m x 1.29 m each) divided by the sample and connected by the air recirculation system, used to generate an airflow through the sample, if needed. The operative temperature is set separately in each chamber, by means of a dedicated hydronic system providing both heating and cooling through radiant panels inside the boxes. The range of operative conditions achievable is between 15°C and 50°C. The control system of the facility is able to maintain the set operative temperatures with a mean squared error below 0.1 °C (Alongi et al. 2017). The sample is accommodated in a 1.5 m x 1.5 m metal frame interposed between the chambers and provided with thermal insulation, in order to minimize any edge effect. The apparatus is supplied with two different frames: one is used to test regular 1 m x 1 m building walls with a maximum thickness of 30 cm, while the other one is dedicated exclusively to test 1.1 m x 1.1 m pneumatic cushions samples as in the present study. The measurement and control system in the DAVTB apparatus is based on an Agilent 34980A multifunctional switch unit, remotely controlled through a LabVIEW algorithm. As far as temperature measurements are concerned,

they are sampled in various points of the hydraulic plant and in various locations inside each chamber, using T-type calibrated thermocouples (TC) with a resulting accuracy of 0.2°C. A globe thermometer with a diameter of 4 cm is installed in the geometrical center of each chamber to measure directly the operative temperature.

The thermal resistance of the cushion is measured through the heat flow and surface temperatures method, as in (GOST 26602.1-99). According to this method, heat flow density and surface temperatures should be measured at different points of the sample surfaces which are representative of an area with homogeneous properties. In this paper, the homogeneous parts are identified with the help of infrared thermography, as described in section 3. Therefore, 32 thermocouples and 16 heat flux meters (HFM) are installed on the sample surfaces to map temperature and heat flux density distribution. Moreover, in order to guarantee a good thermal contact between the probes and the cushion surface, a proper amount of thermally conductive paste was used, namely the minimum amount allowing to remove any air gap between the probes and the cushion surface without altering local heat transfer. The HFMs are 5 gSKIN®-XM 26 9C (sensing dimensions 4.4 mm x 4.4 mm) and 11 gSKIN®-XI 26 9C (sensing dimensions 18.0 mm x 18.0 mm), with a ±3 % calibration accuracy according to the manufacturer GreenTeg. The smaller HFM are used to map the more curved areas of the cushions surface, while the others are placed in the more planar portions.

In order to experimentally assess the thermal resistance of the two cushion samples, a constant operative temperature difference across the sample is established, reproducing the design winter condition in Milan i.e. $\Delta T = 25$ °C, by setting 20 °C in Box 1 and 45 °C in Box 2. Operative temperature in each chamber, cushion surfaces temperature and heat flux density data have been collected every 5 s for a time period of at least 12 h, in order to obtain a stable

set of data that could confirm the steady-state hypothesis and a considerable number of instantaneous data to average.

3 The samples

Double and triple layer configurations have been investigated, i.e. SAMPLE01 and SAMPLE02 respectively. PVC coated polyester fabrics with grammage of 700 g/m^2 and 900 g/m^2 are used on both cases to replicate the inner and the outer surfaces of a real cushion. For the triple layer cushion, another 700 g/m^2 layer is inserted as the central one. FTIR spectrophotometry s used to characterize the fabric thermal emissivity, resulting in $\varepsilon = 0.85$. Both cushions are kept inflated at an internal extra-pressure of 300 Pa using an intermittent air compressor and an external buffer to avoid frequent on/off of the compressor (Figure 2).

For both cushions analyzed, the section is double ogive shaped with a flatter region in the central section and steep tapering toward the edges (see Figure 2). Due to this feature, temperature and heat flux density are expected to vary significantly throughout the surfaces. Therefore, a mapping approach, based on subdividing the surfaces into thermally homogeneous portions and measuring the temperature and heat flux density in the center of each portion, was adopted. Infrared thermography was preliminarily used to help identifying the portions; an example is given in Figure 3, where the temperature distribution on approximately one fourth of the cool side of the sample cushion is shown. It has to be remarked that the IR images were used to highlight the temperature variations on the surfaces, rather than to achieve a measure of the surface temperature distribution itself.

Figure 2: the double layer cushion accommodated in the metal frame and the air inflation system; the central section of the cushion is also depicted.

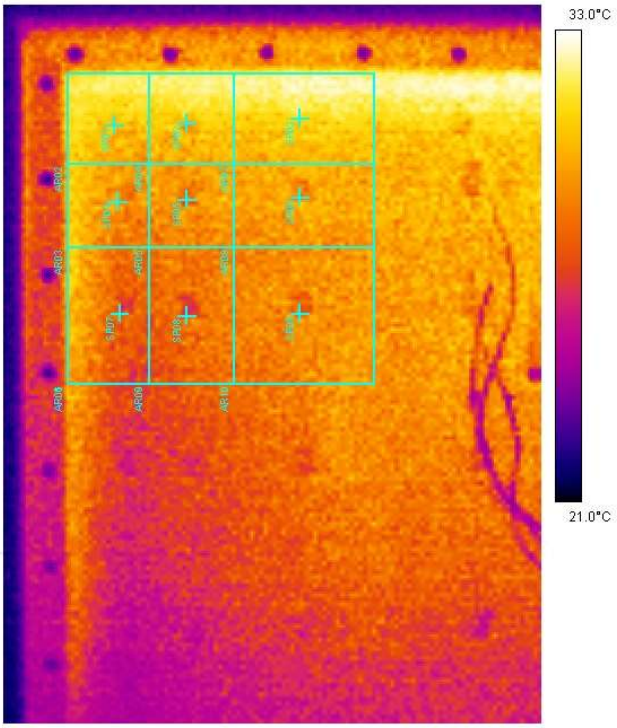

Figure 3: infrared image of the one fourth of the cushion surface (top, cool side). Temperature variation between the centre and the edges can be appreciated.

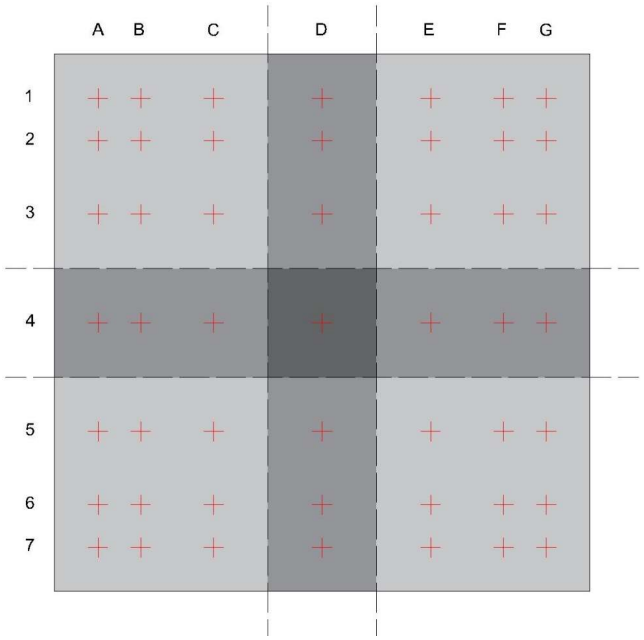

Figure 4: location on a general sample surface of the probing points. Overlapping areas are also visible.

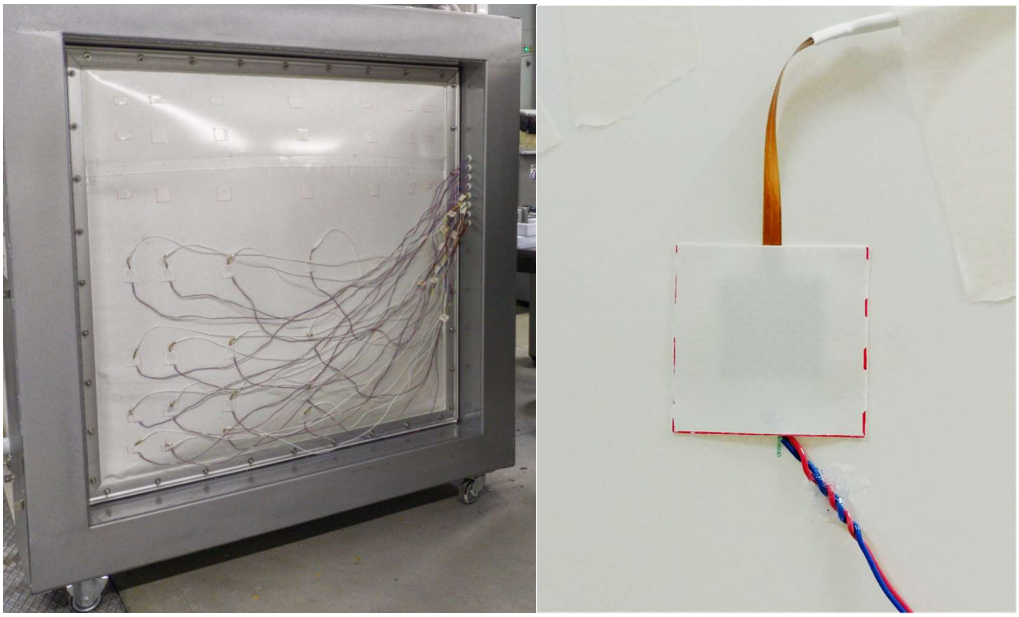

Figure 5. Left: the inflated SAMPLE01 (surface facing Box 2). Thermocouples and heat flux meters location (rows 4-7, columns A-D) is also visible. Right: the probes location with the fabric patch used to match the emissivities of the HFM and the fabric.

Finally, the surfaces of the samples have been divided into 49 portions, with decreasing dimensions going from the center toward the edges (Figure 4). Surface temperatures and heat flows have been measured in the centers of each portion, indicated by the red crosses in Figure 4. Since the measured thermal emissivity of the heat flow meters is equal to 0.65, they are not matched in emissivity with the cushion materials. Therefore, HFMs have been covered with dedicated patches of the same textile material used to produce the cushions, to guarantee that they are subjected to the same radiative conditions of the investigated sample (Figure 5).

As it is possible to infer from Figure 5, the available number of probes is not enough to cover the overall area in a single test. Therefore, the testing procedure applied to each cushion has been divided into four phases, in which temperatures and heat flux densities are measured on corresponding 4 rows-by-4 columns portions of the surfaces, as exemplified in Figure 4:

- phase 1 - from A1 to D4 on the Box 1 side and from D1 to G4 on the Box 2 side;
- phase 2 - from D1 to G4 on the Box 1 side and from A1 to D4 on the Box 2 side;
- phase 3 - from D4 to G7 on the Box 1 side and from A4 to D7 on the Box 2 side;
- phase 4 - from A4 to D7 on the Box 1 side and from D4 to G7 on the Box 2 side.

In this way, both the surfaces are covered completely, with data collected twice on column D and row 4 on both sides and four times on the D4 region. This redundancy allows to verify that the same surface conditions have been achieved in different phases of the test, and thus all the collected data are coherent and can be treated as if they were gathered in a single test.

4. The data processing

This section explains how the cushions thermal resistance is derived from measurements (R_{exp}) and calculated from a simplified physical model (R_{calc}).

Once a steady regime has been reached in each phase, the time average of the following measured quantities is calculated:

- the operative temperature $T_{op,1}$ for Box 1 and $T_{op,2}$ for Box 2;
- the surface temperature $T_{i,j,k}$ on each mapping point of both the sample surfaces, where, according to Figure 4, i represents the column (from A to G), j represents the row (from 1 to 7) and k represents the side of the sample (1 for the surface facing Box 1, 2 for the one facing Box 2);
- the heat flux density $\varphi_{i,j}$ on each mapping point of the surface facing Box 2.

Those quantities that have been measured in more than one phase of the test have then been further averaged over the phases.

Subsequently the area weighted averages of surface temperatures and heat fluxes have been calculated as:

$$\overline{T}_k = \frac{\sum_{i=A}^{G}\sum_{j=1}^{7} A_{i,j}T_{i,j,k}}{\sum_{i=A}^{G}\sum_{j=1}^{7} A_{i,j}} \text{ (average surface temperature toward Box } k\text{)} \qquad (1)$$

$$\overline{\varphi} = \frac{\sum_{i=A}^{G}\sum_{j=1}^{7} A_{i,j} \cdot \varphi_{i,j}}{\sum_{i=A}^{G}\sum_{j=1}^{7} A_{i,j}} \text{ (average heat flux density toward Box 2)} \qquad (2)$$

where $A_{i,j}$ is the area surrounding the i,j mapping location on the sample surface. This comes from the hypothesis of thermal homogeneity over a given i,j area, and allows to mitigate any edge effect or singularity. The overall experimental thermal resistance of the cushion is then calculated as follows:

$$R_{exp} = \frac{\overline{T_2} - \overline{T_1}}{\overline{\varphi}} \qquad (3)$$

The experimental thermal transmittance, that takes into account implicitly the surface heat transfer coefficients in the apparatus, is evaluated from the average values of operative temperatures and the average heat flux density calculated through (2), i.e.:

$$U_{\exp} = \frac{\overline{\varphi}}{T_{op,2} - T_{op,1}} \tag{4}$$

At the same time, using the standard values for the surface heat transfer coefficients (h_{ext} and h_{int} equal to 25 W/(m^{2}K) and 7.7 W/(m^{2}K) respectively), the standard thermal transmittance is calculated as:

$$U_{std} = \frac{1}{\frac{1}{h_{ext}} + R_{\exp} + \frac{1}{h_{\text{int}}}} \tag{5}$$

Besides, the thermal resistances of the two cushions are also calculated considering the heat transfer in the air cavities in parallel by free convection and radiation and disregarding the negligible conductive resistance of the very thin fabric layers:

$$R_{calc,SAMPLE01} = \frac{1}{h_{rd,cav} + h_{cv,cav}} \tag{6}$$

$$\mathrm{R_{calc,SAMPLE02}} = \frac{1}{\mathrm{h_{rd,cav1} + h_{cv,cav1}}} + \frac{1}{\mathrm{h_{rd,cav2} + h_{cv,cav2}}} \tag{7}$$

where $h_{rd,cav}$ and $h_{cv,cav}$ are the radiative and convective heat transfer coefficients in the rectangular cavities, respectively. The first is calculated assuming the two layers are planar parallel grey surfaces at uniform temperatures as:

$$h_{rd,cav} = \frac{4 \cdot \sigma \cdot T_m^4}{\frac{1}{\varepsilon_1} + \frac{1}{\varepsilon_2} - 1} \tag{8}$$

where σ is the Stefan-Boltzmann constant, T_m is the average between the two surface temperatures, ε_1 and ε_2 are the thermal emissivities of the two surfaces. The convective heat transfer coefficient is calculated as a function of the Nusselt number (Nu) as:

$$h_{cv,cav} = Nu \cdot \frac{\lambda_{air}}{s_{cav}} \tag{9}$$

where λ_{air} is the air thermal conductivity evaluated at T_m and s_{cav} is the cavity thickness. Nu is then calculated alternatively using two correlations, therefore resulting in two different values for R_{calc}. The first one is reported in (CEN EN 673, 2011) and is used as technical standard to deal with vertical cavities:

$$Nu = 0.035 \cdot \left(Gr \cdot \mathrm{Pr}\right)^{0.38} \tag{10}$$

where Gr and Pr are the Grashof and Prandtl numbers respectively, calculated as:

$$Gr = \frac{g \cdot \beta \cdot \Delta T \cdot s_{cav}^3}{\nu_{air}^2} \tag{11}$$

$$\mathrm{Pr} = \frac{\nu_{air} \cdot \rho_{air} \cdot c_{p,air}}{\lambda_{air}} \tag{12}$$

with g is the gravity acceleration (9.81 m/s^2), β is the thermal expansion coefficient of air defined as $1/T_m$, ΔT is the difference between surface temperatures, ν_{air}, ρ_{air} and $c_{p,air}$ are the air kinematic viscosity, density and specific heat at constant pressure respectively, all evaluated at T_m. The second is the Berkovsky-Polevikov correlation reported in (Incropera et al., 2007):

$$Nu = 0.22 \cdot \left(\frac{\mathrm{Pr}}{0.2 + \mathrm{Pr}} \cdot Gr \cdot \mathrm{Pr} \right)^{0.28} \left(\frac{h}{s} \right)^{-\frac{1}{4}} \quad (13)$$

where h is the height of the cavity. The validity ranges for this correlation are $Pr < 10^5$, $h/s = 2 \div 10$ and $Gr \cdot Pr = 10^3 \div 10^{10}$.

5. Results and Discussion

Steady state conditions have been established with good accuracy across the samples, since for both tests the standard deviation of the boundary conditions lies in the range 0.03 °C ÷ 0.09 °C, namely within the accuracy of the globe thermometers (~ 0.15 °C).

5.1 Temperature distribution

Figure 6 shows the surface temperature maps for SAMPLE01 (top) and SAMPLE02 (bottom) obtained from the time-averaging process of the measurements.

First of all, a thermal stratification can be noticed, with temperature rising from the bottom to the top of the sample surfaces. Focusing on the central column D (Figure 7) for SAMPLE01 the temperature increases by 3.2 °C on the surface towards Box 1 and by 2.9°C on the surface toward Box 2. Similar results are obtained for SAMPLE02, for which the temperature increase from bottom to top on the central column D is 3.0°C on the Box 1 side and 3.8°C on the Box 2 side. The main reason for these trends is the free convection inside the cavities since the thermal layering in both chambers is less relevant (along the cushion height the air temperature increases by 0.9°C in Box 1 and by 1.3°C on Box 2). It can also be noticed that the temperature variations are mainly located toward the edges, probably due to the shape of the sample section, as it is represented in Figure 1.

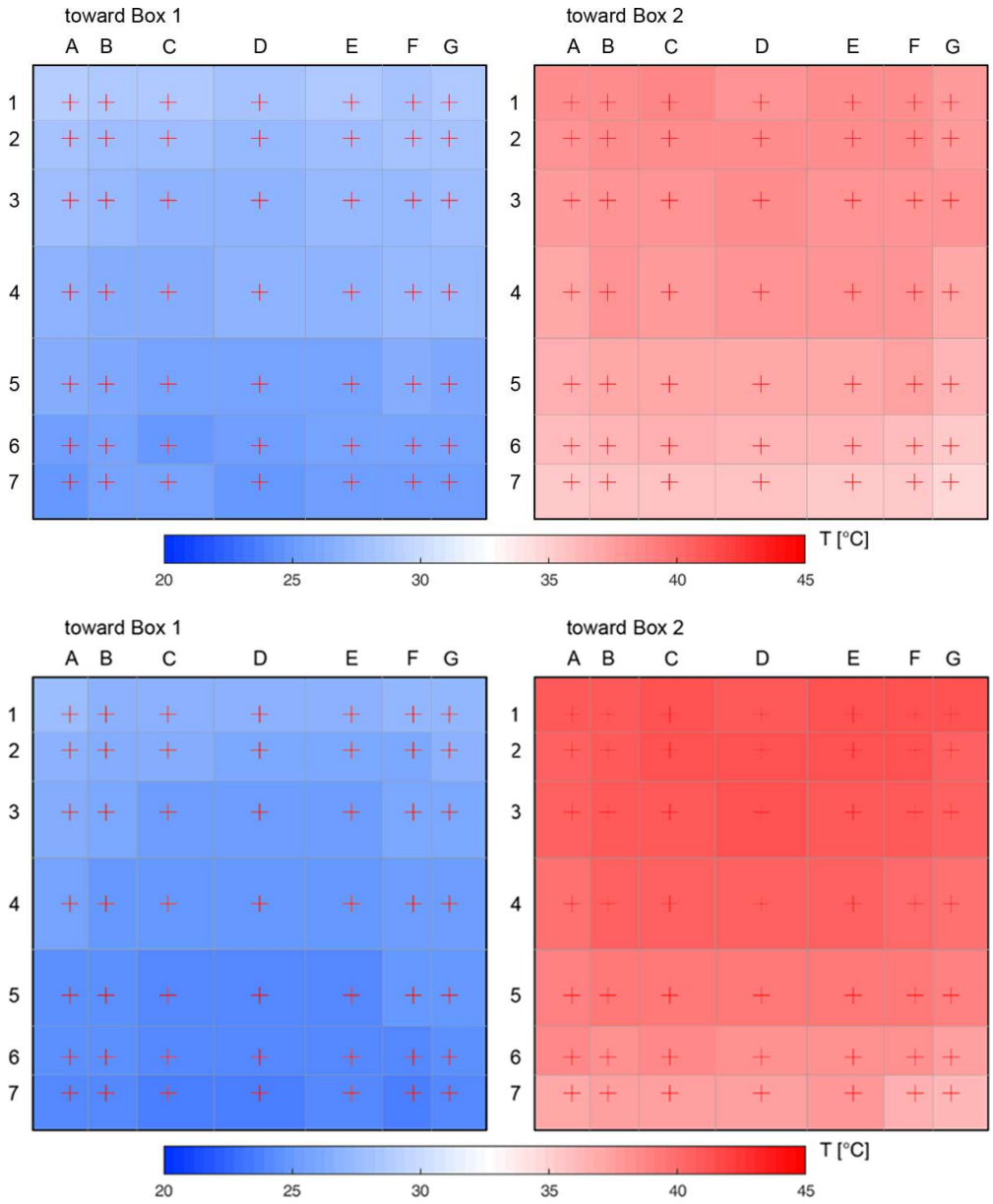

Figure 6: average surface temperature for both the surfaces (toward Box 1 and Box 2) obtained after the experimental investigation of SAMPLE01 (double layer, top) and SAMPLE 02 (triple layer, bottom).

Considering now the temperature variations along the cushion width, at a given height, Figure 6 shows that they are generally less pronounced than along the cushion height. Along the central row 4, on the sample surface toward Box 2 the temperature decrease from the centre to

the edge is 1°C for SAMPLE01 and 0.9°C for SAMPLE02. It can be remarked that some 3D effects are present, although not dominating.

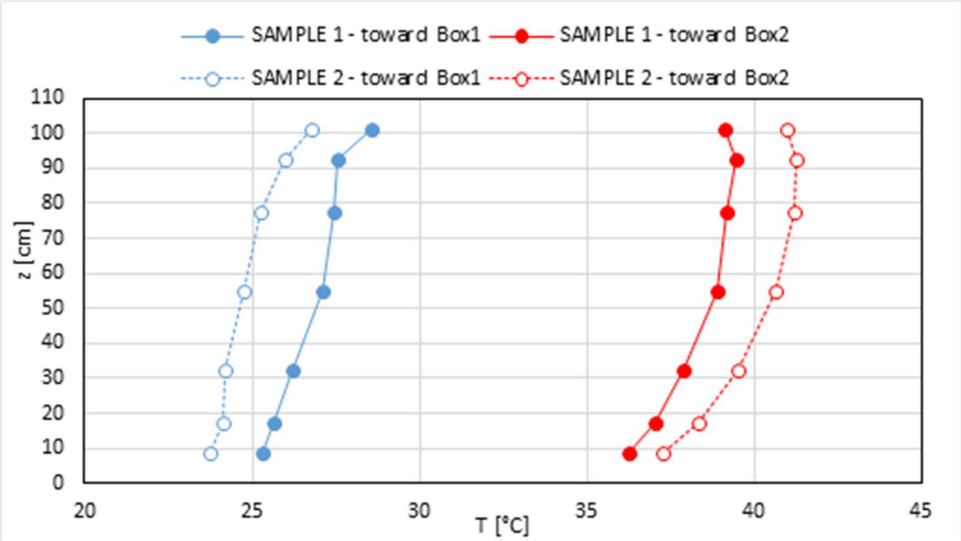

Figure 7: surface temperature versus height (toward Box 1 and Box 2) on the central column D for SAMPLE01 (double layer cushion) and SAMPLE02 (triple layer cushion).

5.2 Experimental thermal resistance and transmittance

Table 1 shows for each cushion sample the average boundary conditions, the average surface temperatures and the average heat flow density, while Table 2 reports the key thermal-physical parameters of the cushions derived from measurements.

Table 1: average boundary conditions and weighted averages of surfaces temperatures and heat flow densities resulting from the tests performed on SAMPLE01 and SAMPLE02.

sample	$T_{op,1}$ **°C**	$T_{op,1}$ **°C**	ΔT_{op} **°C**	$\overline{T}_1$ **°C**	$\overline{T}_2$ **°C**	$\Delta\overline{T}$ **°C**	$\overline{\varphi}$ **W/m²**
01	20.0	45.0	25.0	27.0	38.1	11.1	61
02	20.0	45.0	25.0	25.2	39.8	14.6	42

Table 2: Experimental thermal resistance, experimental transmittance and standard transmittance derived from tests for double and triple layer cushions.

sample	R_{exp} m^2K/W	U_{exp} $W/(m^2K)$	U_{std} $W/(m^2K)$
01	0.183	2.43	2.83
02	0.351	1.67	1.92

Under the same boundary conditions, the heat transfer through the triple layer cushion is 31% less than through the double layer one. The thermal resistance R_{exp} reported in Table 2 is equal to (0.183 ± 0.009) m^2K/W and (0.351 ± 0.015) m^2K/W for the double and the triple layer sample respectively, with expected combined errors equal to 4.8 % and 4.4 %. Although the overall thickness of the sample increases only slightly when passing from two to three layers, namely the configuration passes from one larger to two thinner cavities, the overall thermal resistance of the cushion almost doubles (+ 91%). This might be explained by the reduction of the average thickness of the cavity that partially inhibits the convective motions, therefore reducing the heat transfer, as demonstrated also by the reduction of the average heat flux density and the rise of the average surface temperature difference. In terms of thermal transmittances (Table 2), the triple layer cushion *U*-value is about 30 % lower than the double layer *U*-value. The laboratory thermal transmittance U_{exp} is generally lower than the standard one U_{std}, meaning that convective-radiative heat transfer coefficients in the boxes are lower than the standard ones. Indeed the purpose of the experimental measurements is mainly to compare the performances of the two cushions, rather than deriving *U*-values according to standard conditions.

5.3 Comparison between experimental and calculated thermal resistances

By adopting air thermal-physical properties according to the thermal conditions observed

during the tests (Table 1), the rectangular cavity convective-radiative thermal resistances R_{calc} have been calculated. Since the thickness of the air cavities in the cushions is variable from the centre to the edges, the thickness of the equivalent rectangular cavity can be treated as a parameter. Therefore, R_{calc} have been calculated as a function of the cavity thickness. The analysis has been performed within the range of validity and results are only taken into account when Nu > 1, namely when free convection is active. The results of the calculations are reported in Figure (red lines based on the Berkovsky-Polevikov correlation, blue lines based on the technical standard). For the triple layer sample, the cavity thickness indicated in Figure 8 refers to each of the two cavities. For the sake of comparison the experimental values R_{exp} are also reported as constants (black lines).

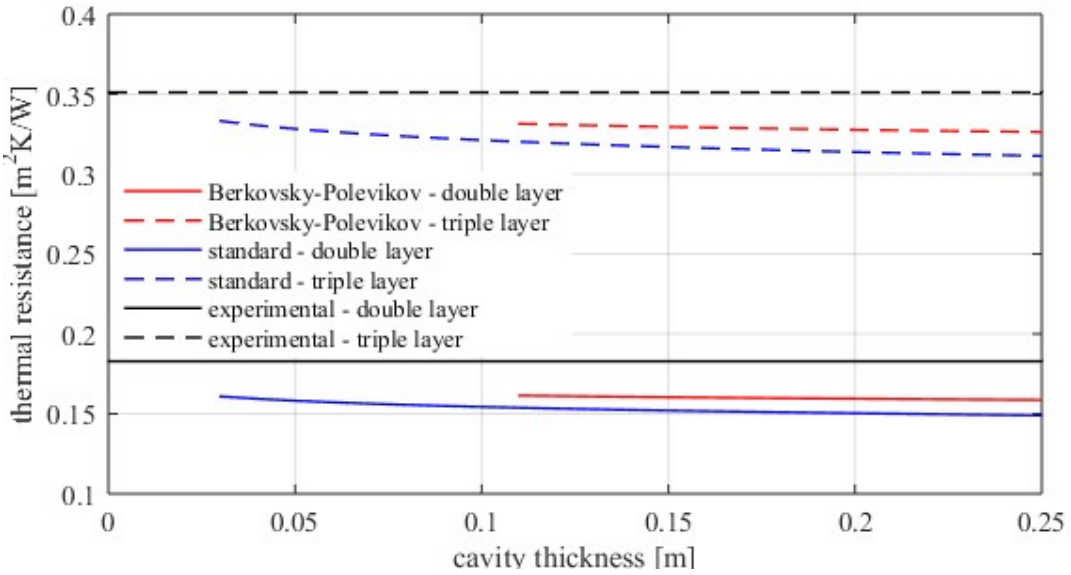

Figure 8: comparison between the experimental thermal resistances, obtained for both Box 1 and Box 2, and the results achieved using correlations from literature for vertical rectangular cavities.

As Figure 8 shows, calculations tend to underestimate the thermal resistances in both double and triple layer samples, with a slightly lower discrepancy for the thermal resistances calculated on the base of Berkovsky-Polevikov correlation (Eq. (13)). If the rectangular cavity

thickness is set equal to the average air gap thickness in real cushions, namely 19 cm for the double and 11 cm for the triple layer sample, the underestimation amount to 13-18 % and 6-9 % for double and triple layers respectively, where the range depends on the natural convection correlation adopted. The discrepancy between measured and calculated values is thus larger than the measurement accuracy, estimated as less than 5%. Moreover, it can be noticed that it is not possible to find any equivalent thickness that allows to represent the heat transfer across a cushion with a vertical cavity with parallel surfaces. A possible explanation might be that the peculiar shape of the sample sections, with the tapering edges, significantly diverges from the simplified models geometry, based on rectangular cavities. CFD simulations, similarly to the ones performed by (Antretter et al., 2008) for comparing horizontal and inclined cushions, will be carried out as a prosecution of this study, in order to understand the impact of the cushion shape on the development of natural convection, in comparison with the classical rectangular cavity. Another possible contribution to the mismatch between measured and calculated thermal resistances may come from the assumption of uniform temperatures on the cushion surfaces, at the basis of the radiative coefficient calculation in Eq. (8), which is not verified during the experiments (Figure 6 and 7).

6. Conclusions

In this work a comparison between double layer and triple layer pneumatic cushions in terms of the heat transfer performance is carried out, by taking the effective curved geometry of the cushions into account. To this purpose, an experimental study on two small vertical samples was performed using the DAVTB apparatus, with some adaptations with respect to the original configuration in (Alongi et al. 2017, Alongi et al. 2020). Temperature and heat flux density distributions have been mapped on both surfaces of each sample during steady state tests, and the results allowed to derive the overall experimental thermal resistance of the two

samples, obtaining 0.183 m^2K/W and 0.351 m^2K/W for the double and the triple layer cushion respectively, with an estimated accuracy below 5 % in both cases. This shows that going from a single large cavity to two smaller ones almost doubles the overall thermal resistance of the cushion. Moreover, no center-of-the cushion calculation of the thermal resistance is able to effectively portray the actual behavior of the samples: both free convection correlations adopted tend to underestimate the experimental thermal resistances, for any cavity thickness. This might be due to the unique shape of the sample cross-section, leading to an overall insulating performance better than what predicted by the simplified models behind the calculations.

Several prospects of this work can be outlined: first of all, new samples will be experimentally investigated, possibly introducing textile materials provided with low emissivity coatings, with the aim to develop more performing pneumatic cushions; secondly, tests will be performed under different operative temperature difference across the samples, reproducing the cushions thermal behavior under different seasons; finally, the convection inside the cushions will be further investigated by means of CFD simulations, in order to better understand the air motion with respect to what happens inside comparable rectangular cavities and possibly generalize these outcomes to different cushion sizes.

References

Afrin S., Chilton J., Lau B. (2015), Evaluation and Comparison of Thermal Environment of Atria Enclosed with ETFE Foil Cushion Envelope. In: *Energy Procedia*, vol. 78, p. 477-482.

Alongi A., Angelotti A., Mazzarella L. (2017), Experimental investigation of the steady state behaviour of Breathing Walls by means of a novel laboratory apparatus. In: *Building and Environment*, vol. 123, p. 415-426.

Alongi A., Angelotti A., Mazzarella L. (2020), Experimental validation of a steady periodic analytical model for Breathing Walls. In: *Building and Environment*, 168, 106509.

Antretter F., Haupt W., Holm A. Thermal Transfer through Membrane Cushions Analyzed by Computational Fluid Dynamics. 8th Nordic Symposium on Building Physics in the Nordic Countries 2008. Copenhagen, Lyngby, p. 347-354.

CEN EN ISO 6946 (2017), Building components and building elements. Thermal resistance and thermal transmittance. Calculation methods, CEN.

CEN EN 673 (2011), Glass in buildings. Determination of the thermal transmittance (U value). Calculation method, CEN.

Cremers J, Marx H. (2017). 3D-ETFE: development and evaluation of a new printed and spatially transformed foil improving shading, light quality, thermal comfort and energy demand for membrane cushion structures. In: *Energy Procedia*, vol. 122, p. 115-120.

Flor J-F., Sun Y., Beccarelli P., Rowell ., Chilton J., Wu Y. (2019), Experimental study on the thermal performance of ethylenetetrafluoroethylene (ETFE) foil cushions. In: *IOP Conf. Series: Materials Science and Engineering*, vol. 556, 012004.

Gomez-Gonzalez A., Neila J., Monjo J. (2011), Pneumatic skins in architecture. Sustainable trends in low positive pressure inflatable systems. In: *Procedia Engineering*, vol. 21, p. 125-132.

Hu J., Chen W., Zhao B., Song H. (2014), Experimental studies on summer performance and feasibility of a BIPV/T ethylene tetrafluoroethylene (ETFE) cushion structure system. In: *Energy and Buildings*, vol. 69, p. 394–406.

Hu J., Chen W., Qiu., Zhao B., Zhou J., Qu Y. (2015), Thermal performances of ETFE cushion roof integrated amorphous silicon photovoltaic, In: *Energy Conversion and Management*, vol. 106, p. 1201-1211.

Hu J., Chen W., Cai Q., Gao C., Zhao B., Qiu Z., Qu Y. (2016), Structural behavior of the PV-ETFE cushion roof. In: *Thin-Walled structures*, vol. 101, p. 169-180.

Incropera F., Dewitt D., Bergman T., Lavine A. (2007), *Fundamentals of Heat Transfer*, 6th ed, John Wiley and Sons, USA.

Interstate Standard of Russian Federation GOST 26602.1-99 (1999), Windows and doors. Methods of determination of resistance to thermal transmission.

Le Cuyer, A. (2008) *ETFE: Technology and Design*, Birkhauser.

Liu H., Li B., Chen Z., Zhou T., Zhang Q. (2016), Solar radiation properties of common membrane roofs used in building structures. In: *Materials and Design,* vol. 105, p. 268–277.

Knippers J., Cremers J., Gabler M., Lienhard J. (2010), *Construction Manual for Polymers + Membranes*, Birkhauser, Basel, Switzerland.

Mainini A.G., Poli T., Paolini R., Zinzi M., Vercesi L. (2012), Transparent multilayer ETFE panels for building envelope: thermal transmittance evaluation and assessment of optical and solar performance decay due to soiling. In: *Energy Procedia*, vol. 48, p. 1302-1310.

Ostrach S. (1972), Natural convection in enclosures, in Hartnett J.P. and Irvine T.F. Eds, *Advances in Heat Transfer*, vol. 8, p. 161-227, Academic Press, New York, USA.

Robinson-Gayle S., Kolokotroni M., Cripps A., Tanno S. (2001), ETFE foil cushions in roofs and atria. In: *Construction and Building Materials*, vol. 15 (7), p. 323–327.

Suo H., Angelotti A., Zanelli A. (2015), Thermal-physical behaviour and energy performance of air-supported membranes for sports halls: a comparison among traditional and advanced building envelopes. In: *Energy and Buildings*, vol. 109, p. 35-46.